International Journal of Science and Research Archive

eISSN: 2582-8185

Cross Ref DOI: 10.30574/ijsra

Journal homepage: https://ijsra.net/

(Review Article)

Check for updates

High-frequency tunable integrated optoelectronic oscillator for advanced communication systems

Md. Ziad Hosain [1], Abdullah Al Niloy [1, *] and Md. Siddik [2]

[1] *Department of Electrical and Electronic Engineering, Canadian University of Bangladesh (CUB) Dhaka 1212, Bangladesh.*
[2] *Department of Electrical and Electronic Engineering, Independent University, Dhaka 1212, Bangladesh.*

International Journal of Science and Research Archive, 2026, 19(02), 224-230

Publication history: Received on 25 March 2026; revised on 04 May 2026; accepted on 07 May 2026

Article DOI: https://doi.org/10.30574/ijsra.2026.19.2.0961

Abstract

Microwave signals that have high spectral purity, and high frequency & frequency tunability, along with microwave generators that are lightweight, compact in size, energy-efficient, and inexpensive, are becoming increasingly in demand as a result of the swift enhancement of modern world communication applications, radar, and wireless systems. To address these expectations, integrated microwave photonics (IMWP) is being considered as a potential solution. The way this is done is by combining the chip's photonics and microwave circuitry. In this work, we both describe and demonstrate an experimental implementation of an integrated optoelectronic oscillator (IOEO). All of the components that are required for the oscillation loop circuit are integrated on a chip monolithically that falls within the dimensions of 5×7 $\boldsymbol{cm^2}$ in size. When the actual injection current is tuned to 45 milliamperes, the output frequency of the prospective IOEO is found to be 7.40 gigahertz, and the noise value of the phase is 92 decibels per hertz at one megahertz. The produced frequency can be altered to 8.9 GHz with a noise value of phase of 90 dBc/Hz@1MHz when the overall injection current is escalated to 65 mA. This is possible when the injection current is increased. Through the use of the injection current, it is possible to make modest adjustments to both of the oscillation frequencies within a range of 22 MHz around the centre oscillation frequency. An in-depth discussion of the approach that can be taken to enhance the performance of IOEO can be found in this article.

Keywords: Integrated Optics; Optoelectronics; Integrated Op-Toelectronic Circuits

1. Introduction

To carry out the changeover between wired signals and wireless, applications that rely on the interfacing between optical fiber and RF signals network segments require devices that are flexible, agile, and compact [1]. Including but not limited to global wireless communications of the fifth generation (5G), radar-based civil surveillance. In addition, there is a pressing need for radio frequency (RF) systems that have a greater degree of complexity, and a wide frequency range which is tunable in the fields of signal creation and processing. Microwave Photonics (MWP) is an area of study that strives to improve the design and execution of optoelectronic systems (hybrid) that are capable of meeting the aforementioned targets [2]. To be more specific, communication networks of pure, are currently undergoing the 5G revolution that intends to service approximately billions of people in the medium-term perspective. Because there is a limited amount of spectrum available at microwave frequencies, basically 5G networks will need to set off at and cover many sorts of regions of the millimeter wave spectrum within the RF bandwidth [3]. Moreover, the characteristics that are anticipated to be present in 5G networks will necessitate the use of millimeter wave sources that possess a high degree of spectral purity, and the ability to tune frequencies. Reduced power usage, a proper design, and a very tiny footprint are all needs that will need to be met to fulfil these objectives. It is proposed that integrated microwave photonics (IMWP) be developed by merging integrated photonics technology [4]. This would allow it to fulfil the

* Corresponding author: Abdullah Al Niloy

requirements that have been outlined above [5]. Because of its capacity to produce high-frequency signals with extremely low phase noise, the optoelectronic oscillator (OEO) is regarded as the best choice among the several approaches that have been reported for the generation of millimeter waves [6]. The first OEO scheme was introduced in 1996, and since then, several different ideas have been developed to realize and improve upon the original OEO scheme. Traditional OEOs often make use of a lengthy fiber delay to achieve a large Q-factor. In an integrated OEO architecture, it is difficult to imagine this capability being implemented in principle [7]. Nevertheless, other illustration initiatives can be utilized to accomplish a large time delay that is accordant with the smaller footprint. A scenario of this would be the high -Q, which was utilized in a miniaturized optical emission oscillator that was published earlier. In this particular design, the 3 optical components of the suggested OEO—the laser, and the detector—inside of a metal box that measured 4×5.6×1.3 cm^3 in volume [8]. The oscillation frequency of this miniaturised OEO could be adjusted, and it had exceptional phase noise values that were lower than 122 dBc/Hz at 100 kHz when the frequency was set to 9.9 GHz. In the most recent years, there have been reports of optical chip-based OEOs that contain optical components that are partially integrated. A high -Q factor for OEO was achieved, for instance, through the utilization of an on-chip-induced Brillouin scattering effect, as described in the reference. It was able to achieve tunability of wideband microwave frequencies while maintaining low-phase noise [9]. We report an integrated optical optical emission spectrometer (IOEO) with an extremely small size in this letter. There is a monolithic integration of all of the photonics components [10]. Additionally, the optical and electrical components are both packaged on a PCB that has a size of 5×7 cm2. Our prototype makes use of a spiral-shaped optical waveguide as a delay line to reduce the amount of phase noise. According to the injection current, the frequency of the IOEO is determined by the current [11]. Tuning the injected current to 45 milliamperes results in an RF frequency of 7.25 gigahertz (1 megahertz) with a noise value (phase) of 89 decibels per hertz at 1 megahertz. When the actual injected current is adjusted to 66 milliamperes, the frequency of the RF that is output is 8.78 gigahertz, and the phase noise value is 92 decibels.

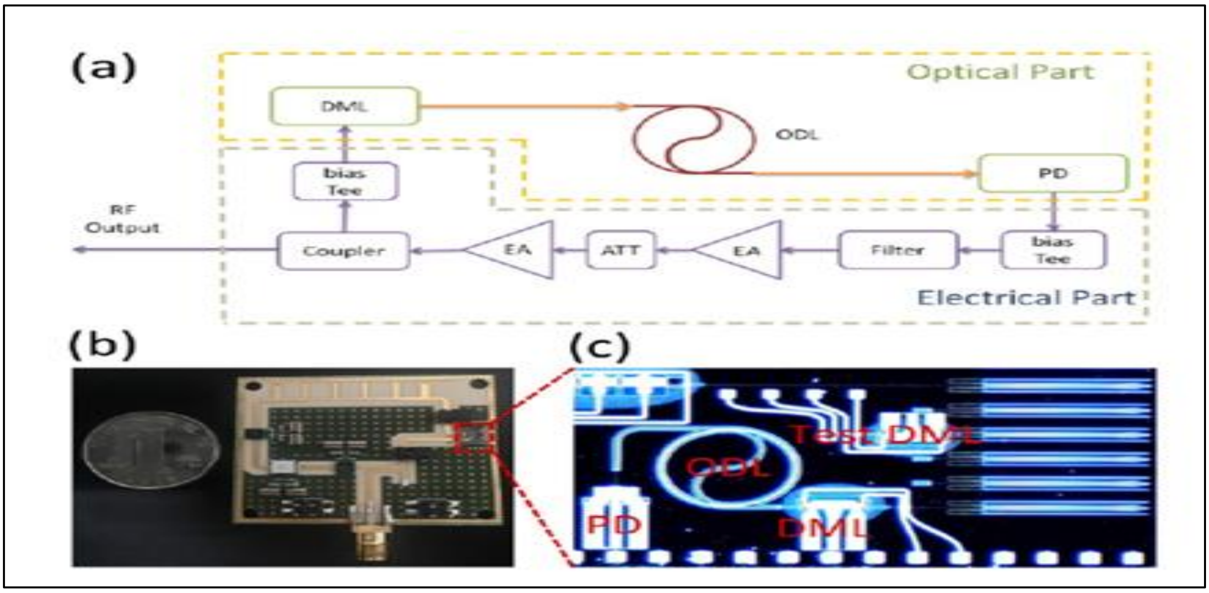

Figure 1 Diagram and picture of the IOEO. (a). Diagram of the suggested IOEO; (b) picture of the completed IOEO; and (c) the photonic component of the IOEO. A photo detector is called a PD; an electrical amplifier is called an EA; an attenuator is called an ATT; and a directly modulated laser is an ODL

This is measured at one megahertz. It is possible to achieve a slight tuning of both oscillation frequencies within a bandwidth of 19 MHz by tightly tuning the injection current [12]. By fully integrating the photonic section and the electrical section on the same board, to the best of our knowledge. We think that this outcome establishes a first and significant milestone on the path toward fully OEO devices [13].

2. Illustration and fabrication

A representation of the proposed IOEO is shown in Fig. 1(a). Figure 1(b) depicts a photograph of the item that was manufactured on the computer. The PD can identify the light wave that originates from the DML after it has passed [14]. Since the phase noise reduces in a manner that is quadratic with the loop time, the ODL is intentionally constructed with a spiral topology to achieve the highest delay duration. The overall ODL is 8.97 millimeters, which is restricted due to the significant loss, which is 2 decibels per centimeter, as well as the size of the chip. After that, the signal that has been detected is put via a microwave filter and an amplifier that can be adjusted. An attenuator that can be adjusted is put into the OEO loop to achieve gain and reduce the amount of gain noise occurring to modulate the DML, one segment is used for feedback [7], which has a power level of ninety percent. In addition, the PCB is equipped with two bias tees to ensure that the DML and PD are driven suitably. In general, the IOEO is made up of an optical component as well as an electrical component. This component is depicted in the right-hand portion of Fig. 1(b), and it is zoomed in during the manufacturing process in Fig. 1(c). On a single printed circuit board (PCB), as depicted in Fig. 1(b), all of the electrical components are assembled. The InP fab at the Fraunhofer Heinrich Hertz Institute (HHI) in Berlin is responsible for the production of the optical chip. We went with a Fe-doped InP wafer, and the cell size is 64 mm2. This is the material that we selected. To create passive components, rib waveguides are utilized. These waveguides are composed of a bulk InGaAsP quaternary core layer, with a bandgap of 1.11 μm [15]. Additionally, there is no additional cladding layer put on the top, making them air-confined. It is a Multi Quantum Well ridge-waveguide structure that serves as the foundation for the DFB laser.

3. Experiments and results

In Fig. 2, the first row represents the findings for an injected current of 51 mA, while the second row portrays the results for an injection current of 59 mA. Both rows are presented in the same order. This may be seen by observing the data shown in these figures. As soon as the injection current reaches a particular threshold, mode competition ensures that only the resonance of the primary mode is preserved. The severe band-pass criteria for the RF filter are reduced when the FSR value is of such a great magnitude [16]. Here, the radio frequency (RF) filter is centered at 11 GHz and has a bandwidth of 9 GHz, which is three decibels, and it can select a maximum of three oscillation modes [17].

The integrated OEO that has been presented can oscillate at numerous frequencies with a variety of injection currents, as demonstrated in Figs. 2(b) and 2(e) [12]. In addition to having an injection current of 45.2 milliamperes, the first stable resonance is 7.30 gigahertz, and it has an amplitude of 0.4 decibel maximum. When the current is tuned to 65 milliamperes, the second one has an amplitude of 0.5 decibels and operates at 8.87 gigahertz. To explain the mechanism of frequency tuning, it is possible to consider the fact that the center laser wavelength grows dramatically with the rising injection current. Consequently, the resonance frequency is raised from 7.28 GHz to 8.78 GHz as a result of the increase in the injection current. When attempting to symbolize the stability of the frequency, the max hold function of the FSA (Tektronix, RSA5126B) is utilized. It is possible to trace this rapid frequency change to the two explanations that are listed below. A further explanation for the significant power discrepancy that can be seen in Fig. 2(b), Fig. 2(e) Fig. 2(c), and Fig. 2(f) is that the oscillation frequency fluctuates at a rapid pace. There is a possibility that the passband of the ESA filter does not contain the point at which the maxi value of the frequency occurs [18]. If this is the case, the power value that was measured and displayed in Fig. 2(c), and Fig. 2(f) is 4.5 decibels less than the result that was measured while the resolution bandwidth was set to 10 megahertz (Fig. 2(b) and Fig. 2(e). It is possible to reduce the fluctuation of the frequency by exchanging the DML for a single-mode laser that is equipped.

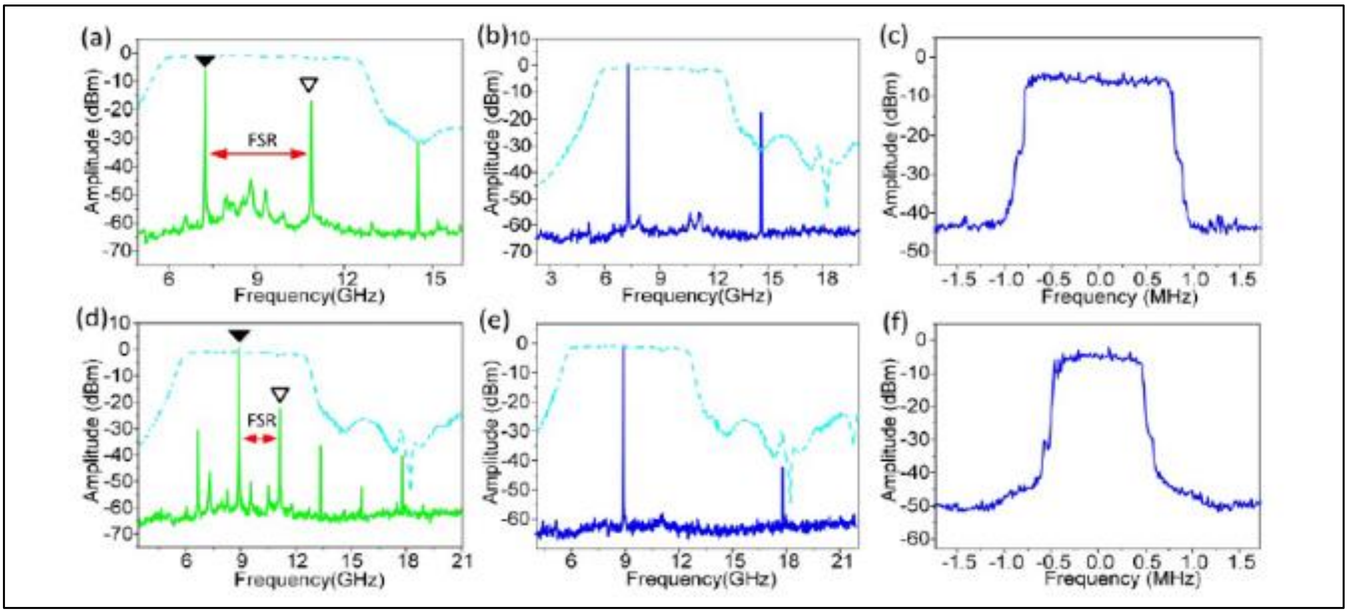

Figure 2 The IOEO's frequency response. The oscillation spectrum for injection currents of 38 mA and 56 mA, respectively, is represented by (a) and (d). The fundamental resonance (second harmonic) is represented by the solid (empty) triangle. (b) The stable output radio frequency spectrum at 33.9 milliamperes of injection current. (c) The principal oscillation frequency fluctuation throughout one minute, as depicted in (b). (e) The frequency spectrum of the steady radio frequency signal is produced at a 65-mA injection current. (f) Variations in the principal oscillation frequency during one minute, as indicated by (e). The resolution bandwidth used to measure the spectrum in (a), (b), (d), and (e) was 11 MHz, whereas (c) and (f) used a resolution bandwidth of 2 KHz. The RF filter's response is shown in (a), (b), (d), and (e) by the cyan dashed line

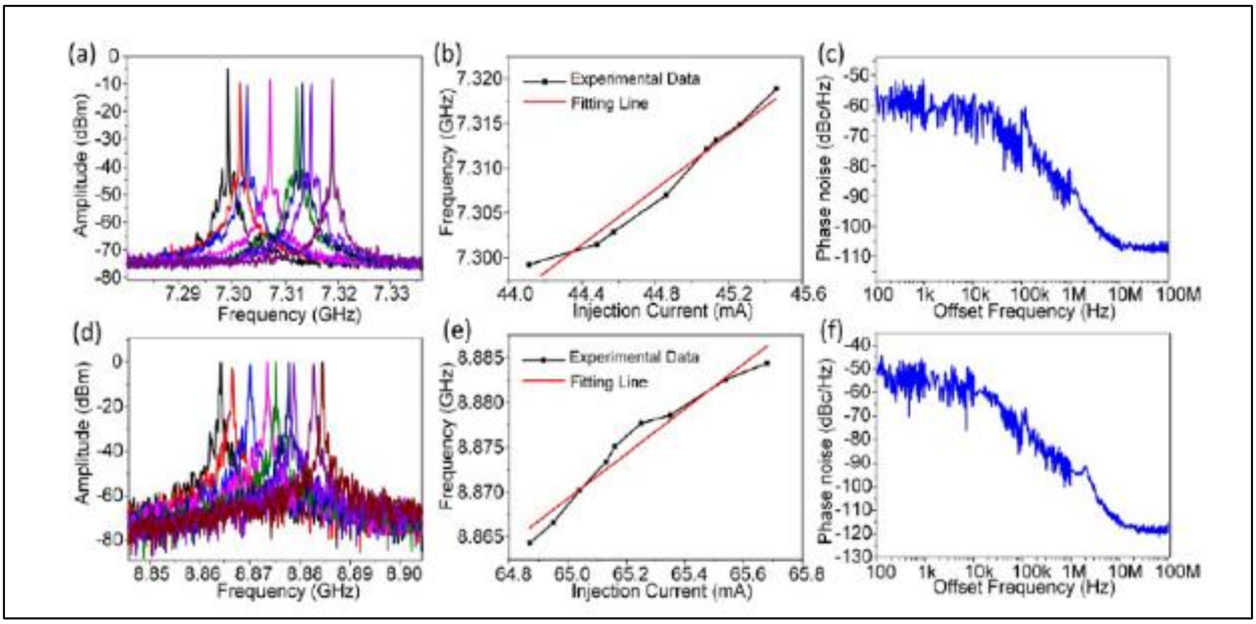

Figure 3 Phase noise response and oscillation frequency tunability of the IOEO. (a), (d), There is tunability for oscillation frequencies between 7.4 GHz and 8.7 GHz. (b) The oscillation frequency is dependent on the injection current at a rate of about 7.4 GHz. (e) The dependence of the oscillation frequency at 8.9 GHz on the injection current is comparable to (b). (c), (f), oscillation frequency phase noise was measured at 7.25 GHz and 8.77 GHz, respectively. While (d) was measured with a resolution bandwidth of 100 KHz, (a) was measured with a bandwidth of 1 KHz

As a potential approach for further stabilizing the oscillation frequency, it is anticipated that controlling the optical chip temp. and the PCB independently will be an effective method. This double frequency is a result of those two factors. The resonance frequency is increased to 9.09 GHz, which results in an improvement to this scenario [19]. In this particular instance, the amplitude of the oscillation is 0.45 dBm, as demonstrated in Fig. 2(e), and the dual component is situated at 18.47 GHz, with an amplitude of 42.2 dBm to be precise. The higher rejection of the RF filter around 17.74 GHz, which can be observed in the RF filter response shown in Fig. 2(e), is the primary source of this phenomenon. This is accomplished by determining the injection current and adjusting it accordingly. It has been determined that the phase noise of the output radio frequency signal is approximately 89 dBc/Hz at 1MHz. Furthermore, when the frequency is adjusted within the continuous frequency tuning range, very slight phase noise variations are seen. This is illustrated in Fig. 3(c). This is demonstrated in Figs. 3(d)-3(f), which displays the same information. The phase noise that was recorded is around 89 dBc/Hz at 1MHz. Ideally, this method for tuning the frequency should be identical to the mechanism for changing the frequency that was described earlier. At the same time that the oscillation frequency is being tuned, mode hopping is prohibited as a result of the huge FSR of the OEO cavity [20]. It can be deduced from the durability of the oscillation that feedback control is an appropriate configuration for the chip.

The instability of high phase noise and oscillation frequency is caused by several constraints that have been recognized in this initial version. These limitations can be summarized into the following points:

3.1. A factor of the oscillation loop that is of low quality

According to the findings of earlier studies, the quality factor Q can be stated as follows:

$$Q = \frac{f_0}{\Delta f_{FWHM}} = \frac{Q_D \tau P_0}{G^2_{A} \rho N} \qquad (1)$$

The oscillation frequency is denoted by f_0, the full-width half-maximum of the oscillation is represented by Δf_{FWHM}, the group delay is denoted by τ, the oscillation power before the RF amplifier is described by $P_0 G^2{}_A$, and the equivalent input noise density is specified as ρN. There, the quality factor of the loop delay is denoted by the equation $Q_D = 2\pi f_0 \tau$. Consequently, the quality factor experiences a quadratic in crease in conjunction with the delay of the loop group. On the other hand, the phase noise of the oscillator, denoted by $L\phi(f)$, the phase noise of the oscillator components, denoted by $L\psi(f)$.

$$L_\phi(f) = \left[1 + \left(\frac{f_L}{f}\right)^2\right] L_\psi(f) \qquad (2)$$

where f represents the offset frequency and f_L represents the Leeson frequency, expressed as $f_L = v_0/2Q$ to be written down. Over here, the oscillation frequency is denoted by vo. When Eq. (1) is taken into consideration, it becomes clear that the extensive group delay has the potential to reduce phase noise by boosting the Q factor. Despite this, the group delay is restricted due to the narrow footprint of the delay line, which increases phase noise.

3.2. Defects that are inherent to the DML The first aspect that has an effect is the RIN that the DML has.

Given that it is difficult to implement temperature control on a chip, the RIN of the laser ought to be high. This will result in a significant increase in the amount of phase noise that is produced. After that, the chromatic dispersion of the InP waveguide that was caused by the enormous frequency noise of the laser that was caused by DML caused a time fluctuation to be induced [21]. The variability in the delay time causes a rapid shift in the frequency of the oscillation, which is ultimately converted into phase noise. This, in turn, leads to a fall in the Q factor, which in turn leads to an increase in phase noise immediately.

3.3. The impact of temperature on the IOEO system

It will be quite difficult to dissipate heat while placing all of the active components, such as the photonics chip, on the printed circuit board (PCB) since it is a thermal material. The condition of each device is impacted by the accumulation of heat that is inherent to the system, in addition to the influence of the environment, which further contributes to the instability of the system [22]. Based on the studies presented above, we can conclude that the four strategies that are listed below should be the primary focus of efforts to enhance the performance of the OEO. To begin with, an increase in the Q factor can be accomplished through the utilization of a whispering gallery mode resonator [23]. Second, to address the shortcomings of the direct modulation mechanism (DML), an external modulation mechanism should be substituted for the direct modulation mechanism [24]. In the third place, thermal control is essential for integrated chips of this kind since it helps to reduce thermal crosstalk and thermal noise. Without the use of a fiber delay line, the phase noise of the OEO was measured to be 122 dBc/Hz at 100 kHz with an oscillation frequency of 8.9 GHz. The proposed

OEO was able to minimize the phase noise by 9 dB. This was accomplished by reducing the laser RIN by 10 to 45 dB over a bandwidth of 9 MHz using the proposed OEO. A phase-locked loop, which is capable of achieving long-term frequency stability, is another method that can be used to realize feedback control [25]. Consequently, we anticipate that the phase noise of the IOEO will be able to reach a level of 115 dBc/Hz at 1 MHz following the upgrade.

4. Conclusion

In conclusion, we present a novel integrated OEO that is formed of two portions on a chip, and we give an experimental demonstration of this integrated OEO. An integrated photonic platform that is based on InP is responsible for the manufacturing of the optical component. It is possible to integrate all of the necessary photonic components into the chip in a monolithic fashion. These components include the ODL, the DML, and the PD. On a single printed circuit board (PCB), the electrical component houses all of the electrical components that are required for the OEO loop. Through the process of tweaking the injection current, we were able to demonstrate that the IOEO is capable of being operated at 2 distinct oscillations with distinct injection currents (7.3 and 8.87 GHz RF, respectively). This is possible in both circumstances. At 7.25 GHz, the phase noise values were measured to be 91 dBc/Hz @1MHz, and at 8.77 GHz, the values were measured to be 92 dBc/Hz @1MHz. Because of the low values of the cavity Q factor and the flaws of the DML, the phase noise value of the signal that is produced by IOEO is larger than the values that are obtained by OEOs that have longer cavities that are implemented by fibers. The strategies that have been discussed and proposed for adoption into future IOEO designs include those that aim to improve the cavity Q factor and increase the oscillation frequency stability. To fulfill the requirements of growing communication, wireless services, and radar application scenarios, integrated technology offers many distinct advantages, including a compact design, a small footprint, a large frequency range needed, and the flexibility to tune the frequency of oscillation.

Compliance with ethical standards

Disclosure of conflict of interest

No conflict of interest to be disclosed.

References

[1] N. J. Gomes, P. P. Monteiro, and A. Gameiro, Next generation wireless communications using radio over fiber. John Wiley & Sons, 2012.

[2] S. Pan and Y. Zhang, "Microwave photonic radars," Journal of Lightwave technology, vol. 38, no. 19, pp. 5450–5484, 2020.

[3] P. Wang, Y. Li, L. Song, and B. Vucetic, "Multi-gigabit millimeter wave wireless communications for 5g: From fixed access to cellular networks," IEEE Communications Magazine, vol. 53, no. 1, pp. 168–178, 2015.

[4] S. Iezekiel, M. Burla, J. Klamkin, D. Marpaung, and J. Capmany, "Rf engineering meets optoelectronics: Progress in integrated microwave photonics," IEEE Microwave Magazine, vol. 16, no. 8, pp. 28–45, 2015.

[5] X. Tang, "Privacy-preserving sensing and wireless communications for iot-enabled smart environments," Ph.D. dissertation, Case Western Reserve University, 2020.

[6] M. A. Ilgaz and B. Batagelj, "Opto-electronic oscillators for micro-and millimeter wave signal generation," Electronics, vol. 10, no. 7, p. 857, 2021.

[7] T. Hao, Y. Liu, J. Tang, Q. Cen, W. Li, N. Zhu, Y. Dai, J. Capmany, J. Yao, and M. Li, "Recent advances in optoelectronic oscillators," Advanced Photonics, vol. 2, no. 4, pp. 044001–044001, 2020.

[8] L. Maleki, "The opto-electronic oscillator (oeo): Review and recent progress," in 2012 European Frequency and Time Forum. IEEE, 2012, pp. 497–500.

[9] K. Saleh, P.-H. Merrer, O. Llopis, and G. Cibiel, "Optical scattering noise in high q fiber ring resonators and its effect on optoelectronic oscillator phase noise," Optics letters, vol. 37, no. 4, pp. 518–520, 2012.

[10] V. Stojanovi´c, R. J. Ram, M. Popovi´c, S. Lin, S. Moazeni, M. Wade, C. Sun, L. Alloatti, A. Atabaki, F. Pavanello et al., "Monolithic silicon photonic platforms in state-of-the-art cmos soi processes," Optics ex press, vol. 26, no. 10, pp. 13106–13121, 2018.

[11] B. Redding, S. F. Liew, Y. Bromberg, R. Sarma, and H. Cao, "Evanes cently coupled multimode spiral spectrometer," Optica, vol. 3, no. 9, pp. 956–962, 2016.

[12] J. Tang, T. Hao, W. Li, D. Domenech, R. Ba˜nos, P. Mu˜noz, N. Zhu, J. Capmany, and M. Li, "Integrated optoelectronic oscillator," Optics express, vol. 26, no. 9, pp. 12257–12265, 2018.

[13] L. Carroll, J.-S. Lee, C. Scarcella, K. Gradkowski, M. Duperron, H. Lu, Y. Zhao, C. Eason, P. Morrissey, M. Rensing et al., "Photonic packaging: transforming silicon photonic integrated circuits into photonic devices," Applied Sciences, vol. 6, no. 12, p. 426, 2016.

[14] Y. Matsui, "Directly modulated laser technology: Past, present, and future," in Datacenter Connectivity Technologies. River Publishers, 2022, pp. 87–171.

[15] M. W. Dashiell, J. F. Beausang, H. Ehsani, G. Nichols, D. M. Depoy, L. R. Danielson, P. Talamo, K. D. Rahner, E. J. Brown, S. R. Burger et al., "Quaternary ingaassb thermophotovoltaic diodes," IEEE Transac tions on Electron Devices, vol. 53, no. 12, pp. 2879–2891, 2006.

[16] Y. Yanagase, S. Suzuki, Y. Kokubun, and S. T. Chu, "Box-like filter response and expansion of fsr by a vertically triple coupled microring resonator filter," Journal of lightwave technology, vol. 20, no. 8, p. 1525, 2002.

[17] M. C. Pennington, Phonology in English language teaching: An international approach. Routledge, 2014.

[18] A. C. Bovik, P. Maragos, and T. F. Quatieri, "Am-fm energy detection and separation in noise using multiband energy operators," IEEE trans actions on Signal Processing, vol. 41, no. 12, pp. 3245–3265, 1993.

[19] M. B. Hossain, M. R. I. Faruque, A. S. Alshammari, and M. T. Islam, "Wide bandwidth enriched symmetric hexagonal split ring resonator based triple band negative permittivity metamaterial for satellite and wi-fi applications," Results in Physics, vol. 37, p. 105511, 2022.

[20] T. Hao, Q. Cen, S. Guan, W. Li, Y. Dai, N. Zhu, and M. Li, "Opto electronic parametric oscillator," Light: Science & Applications, vol. 9, no. 1, p. 102, 2020.

[21] S. Matsuo and T. Kakitsuka, "Low-operating-energy directly modulated lasers for short-distance optical interconnects," Advances in Optics and Photonics, vol. 10, no. 3, pp. 567–643, 2018.

[22] C. Ning, C. S. K. Lin, D. C. W. Hui, and G. McKay, "Waste printed circuit board (pcb) recycling techniques," Chemistry and Chemical Technologies in Waste Valorization, pp. 21–56, 2018.

[23] K. Wei and A. S. Daryoush, "Hybrid modeling and design optimization of chip level of μs long optical delays for realization of integrated optoelectronic circuits." Progress In Electromagnetics Research, vol. 172, 2021.

[24] P. Nagy, "Kinetics and mechanisms of thiol–disulfide exchange covering direct substitution and thiol oxidation-mediated pathways," Antioxidants & redox signaling, vol. 18, no. 13, pp. 1623–1641, 2013.

[25] Grote, M. Baier, and F. Soares, "Photonic integrated circuits on inp," Fibre Optic Communication: Key Devices, pp. 799–840, 2017.